Neutron diffraction determination of magnetic order in holmium trifluoride, HoF_3

1990 J. Phys.: Condens. Matter 2 4471

(http://iopscience.iop.org/0953-8984/2/19/013)

J. Phys.: Condens. Matter 2 (1990) 4471–4484. Printed in the UK

Neutron diffraction determination of magnetic order in holmium trifluoride, HoF_3

P J Brown†, J B Forsyth‡, P C Hansen§, M J M Leask§, R C C Ward§ and M R Wells§

† Institut Laue–Langevin, Grenoble, France
‡ Rutherford Appleton Laboratory, Oxon, UK
§ The Clarendon Laboratory, Parks Road, Oxford OX1 3PU, UK

Received 24 November 1989, in final form 28 February 1990

Abstract. The Ho^{3+} ion ($4f^{10}$, $^5I_8$) in holmium trifluoride has a singlet ground state and an excited state, also a singlet, at 6.59 cm^{-1}. In HoF_3 the nuclear moments (^{165}Ho, $I = \frac{7}{2}$) are strongly enhanced through the hyperfine interaction, and previous results concluded that at $T_N = 0.53$ K the crystal undergoes a transition to an ordered antiferromagnetic state with both nuclear and electronic moments parallel and antiparallel to the orthorhombic a axis. Neutron diffraction studies at temperatures well below T_N have revealed that the ordered magnetic state is at variance with earlier conclusions and is more complex. A refinement of the neutron diffraction data shows that the ordered state may be described as $Pnm'a'$ (F_xC_z) with Ho^{3+} moments of 5.7(2) μ_B at 66 degrees to [001]. The temperature dependence of the the intensities of the [100], [140] and [420] reflections have been determined for $0.07 < T < 0.6$ K and are compared with the predictions of molecular field theory.

1. Introduction

Holmium trifluoride, HoF_3, has an orthorhombic cell with $a = 6.404$, $b = 6.875$ and $c = 4.379$ Å at ambient temperature (Zalkin and Templeton 1953). The space group is $Pnma$ (D_{2h}^{16}) with an eightfold general position: $\pm[(x, y, z); (\frac{1}{2} + x, \frac{1}{2} - y, \frac{1}{2} - z); (-x, \frac{1}{2} + y, -z); (\frac{1}{2} - x, -y, \frac{1}{2} + z)]$. The cell contains four Ho and twelve F atoms positioned as follows:

Atom	Site	Site symmetry	x	y	z
Ho	4c	m	0.3679(1)	$\frac{1}{4}$	0.0614(1)
F1	8d	1	0.1662(6)	0.0645(6)	0.3797(9)
F2	4c	m	0.0224(9)	$\frac{1}{4}$	0.9140(10)

as determined from x-ray single-crystal data by Bukvetskii and Garashina (1977). There are four HoF_3 formula units per unit cell. The low symmetry at the Ho^{3+} sites—C_{1h} (m)—results in the $^5I_8$ ground manifold being split into singlet states. Previous thermal, magnetic and magneto-optical studies of HoF_3 (Bleaney *et al* 1988) have shown that a

0953-8984/90/194471 + 14 $03.50

single-ion model for Ho^{3+}, with an excited state 6.59 cm^{-1} above the ground state, allows a reasonable but not very precise description of a variety of observed magnetic properties at temperatures between 0.5 and 4.2 K. Collectively these results indicated the onset of antiferromagnetic order at $T_N = 0.53$ K, with the holmium moments aligned parallel and antiparallel to the orthorhombic *a* axis. The strong hyperfine interaction in HoF_3 results in the ^{165}Ho ($I = \frac{7}{2}$) nuclear moments being enhanced by a factor of about 600. The nuclear susceptibility therefore provides a necessary addition to the Van Vleck (electronic) temperature independent susceptibility. The Néel temperature (530 mK) for this nuclear-plus-electronic singlet ground state system is higher than for any other rare earth compound so far reported in the literature.

We now report a determination of the magnetic structure of HoF_3 at 70 mK—well below T_N—and the variation with temperature of the nuclear and magnetic order parameters between 530 and 70 mK, the base temperature of the dilution refrigerator.

2. The experiments

A HoF_3 single-crystal grown by the Czochralski method was cut in the form of a right cylinder 10 mm × 3 mm diameter with the *c* axis along the cylindrical axis. The direction of the orthorhombic *a* axis was determined by standard x-ray techniques. The sample was attached to the cold finger of an ILL dilution refrigerator mixing chamber using Stycast resin adhesive. Using normal beam geometry on the D15 diffractometer at ILL, Grenoble, the integrated intensities of 272 ($h\,k\,0$) reflections out to a limit of $\sin\theta/\lambda = 0.85$ $Å^{-1}$ were recorded at 100 K, and 312 intensities at 70 mK. After averaging over equivalent reflections, each data set reduced to 85 unique structure factors with merging *R*-factors of $\mathcal{F}^2$ of some 1.5%.

To determine the temperature dependence of the order parameters below T_N, the intensities of a few selected reflections were studied in detail as a function of temperature in the range 70–600 mK. The time taken to attain thermal equilibrium, especially in the middle of this temperature range, was up to five hours. This was not surprising, as it was expected that the onset of nuclear ordering and the consequent hyperfine splittings would result in a large Schottky heat capacity with a maximum in the temperature range 200–300 mK. At temperatures either side of this range, temperature equilibrium was attained within minutes, testifying to good thermal contact between the crystal and the thermometer. Heating of the crystal due to absorption of the neutron beam was eliminated as a source of temperature uncertainty by showing the (1 0 0) Bragg peak intensity to be independent of the neutron beam intensity in a temperature region where the Bragg peak intensity was a steeply varying function of temperature (350–400 mK), see figure 2 later. The temperature of the mixing chamber was monitored by a calibrated germanium thermometer using a two lead arrangement below the cryostat top plate. A correction was therefore necessary to determine the precise resistance of the thermometer. This correction amounted to +19 mK at 500 mK, and less at lower temperatures.

3. Determination of the magnetic structure

At $T = 100$ K, non-zero intensities were observed for all the recorded reflections ($h\,k\,0$), even those forbidden for the space group P*nma*. These latter were however far less

intense than those allowed by P*nma*, being at the strongest some 1% of the intensity of the strong allowed reflections. Their presence was attributed to multiple scattering, which is to be expected for such a large specimen. At the lowest temperature, $T =$ 70 mK, all the recorded $(h\,k\,0)$ reflections were more intense than at 100 K. Table 1 lists the experimentally determined structure factors $\mathcal{F}_{\text{hot}}$ and $\mathcal{F}_{\text{cold}}$, corresponding to $T =$ 100 K and 70 mK respectively, for reflections with $\sin\theta/\lambda < 0.5$ Å^{-1}. Also listed is the quantity $\mathcal{F}^2_{\text{cold}} - \mathcal{F}^2_{\text{hot}}$ which is proportional to the magnetic scattering below T_N.

Table 1. Calculated $\mathcal{F}^2_M(\tau)$ for Ho^{3+} tons.

(hkl)	F	G	C	A	$\mathcal{F}_{\text{hot}}$	$\mathcal{F}_{\text{cold}}$	$(\mathcal{F}^2_{\text{cold}} - \mathcal{F}^2_{\text{hot}})$
010	0.0	16.0	0.0	0.0	33.0	39.8	498.3
020	16.0	0.0	0.0	0.0	197.6	298.6	50116.2
030	0.0	16.0	0.0	0.0	23.0	26.6	179.0
040	16.0	0.0	0.0	0.0	354.7	388.6	25197.9
050	0.0	16.0	0.0	0.0	43.5	46.0	226.1
060	16.0	0.0	0.0	0.0	497.2	505.6	8423.5
100	0.0	0.0	7.2	8.8	52.5	175.0	27870.8
110	0.0	0.0	8.8	7.2	41.6	180.7	30920.3
120	0.0	0.0	7.2	8.8	30.8	155.3	23172.5
130	0.0	0.0	8.8	7.2	30.7	148.3	21049.2
140	0.0	0.0	7.2	8.8	28.3	121.0	13841.8
150	0.0	0.0	8.8	7.2	30.5	110.0	11170.4
160	0.0	0.0	7.2	8.8	33.5	85.5	6190.0
200	0.2	15.8	0.0	0.0	51.6	55.6	434.3
210	15.8	0.2	0.0	0.0	149.4	249.0	39680.6
220	0.2	15.8	0.0	0.0	290.5	289.8	−406.2
230	15.8	0.2	0.0	0.0	374.6	408.6	26628.8
240	0.2	15.8	0.0	0.0	205.9	208.3	994.1
250	15.8	0.2	0.0	0.0	98.6	257.2	56425.9
260	0.2	15.8	0.0	0.0	44.5	53.4	868.6
300	0.0	0.0	10.4	5.6	42.1	164.3	25217.9
310	0.0	0.0	5.6	10.4	26.1	125.8	15144.4
320	0.0	0.0	10.4	5.6	30.6	150.1	21591.8
330	0.0	0.0	5.6	10.4	48.3	114.7	10821.3
340	0.0	0.0	10.4	5.6	24.3	116.8	13050.3
350	0.0	0.0	5.6	10.4	31.9	82.8	5840.1
360	0.0	0.0	10.4	5.6	28.1	83.3	6146.5
400	15.4	0.6	0.0	0.0	349.5	352.0	1683.8
410	0.6	15.4	0.0	0.0	52.5	57.8	586.7
420	15.4	0.6	0.0	0.0	38.4	160.0	24127.7
430	0.6	15.4	0.0	0.0	404.5	400.7	−3075.9
440	15.4	0.6	0.0	0.0	175.7	241.2	27307.0
450	0.6	15.4	0.0	0.0	196.0	198.7	1065.7
500	0.0	0.0	4.2	11.8	29.4	81.5	5777.9
510	0.0	0.0	11.8	4.2	34.8	116.7	12411.3
520	0.0	0.0	4.2	11.8	41.7	83.3	5198.3
530	0.0	0.0	11.8	4.2	33.5	100.6	8999.4
540	0.0	0.0	4.2	11.8	37.1	67.5	3178.4
600	1.4	14.6	0.0	0.0	488.0	487.3	−682.7
610	14.6	4.4	0.0	0.0	420.5	420.8	252.4
620	1.4	14.6	0.0	0.0	102.0	108.7	1411.7

These data allow immediate conclusions to be drawn regarding the arrangement of the Ho^{3+} moments below T_N, from a qualitative comparison of $\mathcal{F}^2_{cold} - \mathcal{F}^2_{hot}$ with the squared magnetic geometrical structure factors calculated for the four possible configurations of moments in the unit cell. Numbering the four Ho^{3+} ions in the unit cell as

$$1: [x\ \tfrac{1}{4}\ z] \qquad 2: -[x\ \tfrac{1}{4}\ z]$$

$$3: [x + \tfrac{1}{2}\ \tfrac{1}{4}\ \tfrac{1}{2} - z] \qquad 4: -[x + \tfrac{1}{2}\ \tfrac{1}{4}\ \tfrac{1}{2} - z]$$

the four configurations are

	1	2	3	4
F:	+	+	+	+
G:	+	−	+	−
C:	+	+	−	−
A:	+	−	−	+

We use here the notation of Koehler *et al* (1960). *F* corresponds to both the non-magnetic (nuclear) scattering expected at high temperatures, and to ferromagnetic order which may be possible in principle at the lowest temperatures. Table 1 lists the calculated values of the squared magnetic geometric structure factors, $\mathcal{F}^2_M(\tau)$ for the ordering configurations *F*, *G*, *C*, *A* as a function of $(h\,k\,0)$. It is clear from the comparison with the forbidden P*nma* reflections $(1\,k\,0)$, and more particularly $(3\,k\,0)$, that the systematic variation of the experimental data is more consistent with the *C* configuration than with either *A* or *G*.

However, another important feature of the data in table 1 is the increased intensity in the allowed P*nma*, *h*-even reflections at 70 mK. Again, the comparison shows the systematic variation to be consistent with an ordered configuration of type *F*.

This unexpected result (there was no evidence for the onset of ferromagnetic order in the previous experiments of Bleaney *et al* 1988) raises two further matters. First, there is a need to demonstrate that the implied coexistence of *C* antiferromagnetic order and *F* ferromagnetic order—in directions as yet unspecified—is consistent with space group and magnetic group symmetry requirements. Second, since the propagation vectors of *F* and *C* are certainly orthogonal, the direction of the Ho^{3+} moment relative to the crystallographic axes needs to be determined.

We therefore proceed to the group theoretical treatment of the magnetic order in the space group P*nma* (D^{16}_{2h}). The eight symmetry operations in this space group, all of which commute with each other, allow the construction of a table of representations and magnetic groups in P*nma*, as described by Bradley and Cracknell (1972). Each of the eight magnetic space groups associated with P*nma* forms a basis for one of the irreducible representations (reps) in D_{2h}. The assignment of each to the appropriate rep is made by reference to the published tables of magnetic groups (Bradley and Cracknell 1972), and the result is given in table 2.

To relate these results specifically to HoF_3, we assign the four-atom basis functions *F*, *G*, *C*, *A* already given above to the appropriate reps in table 2. In the point group D_{2h} of the space group P*nma* we have to consider just the twelve functions consisting of the *x*, *y* and *z* components of the above four. Using the well known transformation properties of spin functions under space group operations, the twelve spin functions can be assigned to each of the magnetic groups, as listed in the last column of table 2. It can be seen that

Table 2. Representations and magnetic groups in $Pnma(D_{2h}^{16})$.

Reps in D_{2h}	Pnma symmetry operations† 1	2	3	4	5	6	7	8	Magnetic group	Basis functions
Γ_1^+	1	1	1	1	1	1	1	1	$Pnma$	C_y
Γ_2^+	1	−1	1	−1	1	−1	1	−1	$Pn'ma'$ (448)	F_y
Γ_3^+	1	−1	−1	1	1	−1	−1	1	$Pnm'a'$ (447)	F_x, C_z
Γ_4^+	1	1	−1	−1	1	1	−1	−1	$Pn'm'a'$ (446)	F_z, C_x
Γ_1^-	1	1	1	1	−1	−1	−1	−1	$Pn'm'a'$ (449)	G_x, A_z
Γ_2^-	1	−1	1	−1	−1	1	−1	1	$Pnm'a$ (444)	G_z, A_x
Γ_3^-	1	−1	−1	1	−1	1	1	−1	$Pn'ma$ (443)	A_y
Γ_4^-	1	1	−1	−1	−1	−1	1	1	$Pnma'$ (445)	G_y

† As numbered in the *International Tables for Crystallography*.

the four y components are each unique to a particular magnetic group, while the x- and z-components occur in four pairs. This is because (i) the one true mirror plane in $Pnma$ is the plane normal to the y axis, and (ii) there are no principal directions in the x–z plane determined by symmetry. Such directions therefore need to be determined by experiment.

We note also that the ordered configurations F and C co-exist as basis functions for the magnetic groups $Pnm'a'$ (F_xC_z) and $Pn'm'a$ (F_z, C_x). This coexistence implies a canting of the Ho^{3+} moments somewhere in the x–z (a–c) plane. The refinement of the magnetic structure at 70 mK, given below, determines the direction and magnitude of the moment, and also allows a choice to be made between the magnetic groups $Pnm'a'$ and $Pn'm'a$.

We can also conclude from the data in table 1 that the chemical and magnetic unit cells are identical. In particular, it is most unlikely that the magnetic cell is double the chemical unit cell in one or more of the [100], [010], [001] directions. Elementary considerations lead to the prediction that for cell doubling in a particular direction, exact cancellation leading to zero reflection intensity would occur for all reflections in the plane normal to the doubling direction. Thus had the doubling occurred along [001], the magnetic contribution to all the reflections listed in table 1 would have been zero. This is evidently not the case. Correspondingly, doubling along [100] or [010] would have led to zero magnetic intensity for the $(0\,k\,0)$ and $(k\,0\,0)$ reflections respectively; again, this is not the case.

3.1. Refinement of the magnetic structure at 70 mK ($T \ll T_N$)

The intensity in the forbidden $Pnma$ reflections at 100 K was used to make an approximate correction for the multiple scattering in the remaining integrated intensities, and the same corrections were applied to the whole of the 70 mK data. The structure factors were then placed on an absolute scale by a least squares refinement of the 100 K data starting from the positional parameters of Bukvetski and Garashina (1977). The small degree of extinction was modelled by a Lorentzian distribution of mosaic spread in the Becker and Coppens (1974) formalism. The final R-factor was 6.6% for the positional parameters, a temperature factor, a mosaic spread parameter and the scale factor for the 39 allowed $Pnma$ reflections. Due to the relatively few data, it was decided to fix the

isotropic temperature factors of Ho at 0.15 Å^2 and vary an equal isotropic temperature factor on the two fluorine atoms. The final values for the x and y positional parameters (z being unrefinable from the present measurements in the $(h\,k\,0)$ plane) are not much different from the ambient values, being

F1 $x = 0.1652(14)$ $y = 0.0642(8)$

F2 $x = 0.0185(15)$

Ho $x = 0.3688(10)$.

The temperature factor for F1 and F2 was refined to 0.48(6) Å^2. Treatment of the 70 mK data had to take into account that the Ho nuclei are 98(2)% polarised at this temperature. The neutron scattering amplitude for a nucleus with spin s may be written

$$b + 2B\boldsymbol{I} \cdot \boldsymbol{s}.$$

The second term expresses the interaction between the neutron carrying a spin s and the nucleus carrying a spin $\boldsymbol{I}$. In their turn, b and B may be expresed in terms of b_+ and b_-, the scattering amplitudes corresponding to scattering by the $I + \frac{1}{2}$ and $I - \frac{1}{2}$ compound states, respectively:

$$b = [(I+1)b_+ + Ib_-]/(2I+1) \qquad B = (b_+ - b_-)/(2I+1).$$

The scattering of unpolarised neutrons by a crystal containing polarised nuclei and ordered electronic moments is proportional to $\mathcal{F}^2$, where

$$\mathcal{F}^2 = N^2 + |\boldsymbol{Q} + CI\boldsymbol{P}|^2.$$

Here N is the nuclear structure factor derived from the values of b, $\boldsymbol{Q}$ the electronic magnetic interaction vector, C the nuclear spin dependent structure factor derived from the values of B, and $\boldsymbol{P}$ is the nuclear polarisation. The cross term $2CI\boldsymbol{Q} \cdot \boldsymbol{P}$ does not average to zero, since both quantities involve the neutron spin operator.

For ^{165}Ho, $(b_+ - b_-)$ is $-0.342(2) \times 10^{-12}$ cm, so that the value of BI for a single nucleus is -0.150×10^{-12} cm which is equivalent to the scattering power of a pseudonuclear moment of $-0.555(3)\ \mu_B$ (see, for example, Glattli and Goldman 1987). In HoF_3, the direction of $\boldsymbol{P}$ will always be either parallel or antiparallel to the direction of the ionic magnetic moment, depending on the sign of the hyperfine interaction. The presence of nuclear polarisation is therefore modelled by including a moment $\pm 0.55\ \mu_B$, with a form factor independent of $\sin\theta/\lambda$, in the description of the magnetic structure. A least squares refinement was carried out using a special program MGILSQ, written using the Cambridge Crystallographic Subroutine (Brown and Matthewman 1987) which allows the structure factors to be calculated taking account of aligned nuclear spins.

The Ho^{3+} electronic form factor was modelled by the $\langle j_0 \rangle$ and $\langle j_2 \rangle$ radial integrals corresponding to the Ho^{3+} free ion relativistic Hartree–Fock wavefunctions of Freeman and Desclaux (1979). In Ho^{3+} $\boldsymbol{L}$ and $\boldsymbol{S}$ couple additively, so that in the dipole approximation the spherically symmetric part of the magnetic scattering will have a form factor which is expanded relative to the spin-only function $\langle j_0 \rangle$ by the addition of a fraction, v, of the function $\langle j_2 \rangle$. For $L = 6$ and $S = 2$ we should expect v to be 0.60 (Johnston 1966), but this factor was kept as a variable in a refinement based on the 85 moduli of structure factors observed at 70 mK. The positional parameters, the scale factor and the mosaic spread parameter were fixed at the values obtained from the refinement of the 100 K data. The nuclear pseudomoment was fixed at $-0.55\ \mu_B$, corresponding to a positive hyperfine field coupling constant. A final R-factor of 6.3%, with $R^W = 4.9\%$, was

obtained with a Ho^{3+} moment of 5.7(2) μ_B at an angle of 66(1)° from [001] (see figure 1). The fraction v, refined to 0.466(6), is somewhat smaller than that corresponding to the simplest estimate of 0.6. Reversing the sign of the nuclear pseudomoment gave a refined value of v which was negative, as might be expected, so this choice could be rejected. Table 3 lists the observed and calculated scale moduli structure factors, and the individual nuclear and magnetic structure factors contributing to the reflections measured at 70 mK.

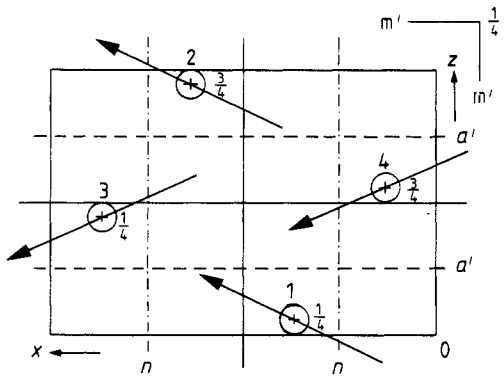

Figure 1. [010] projection of the magnetic structure of HoF_3 showing the relative orientation of the magnetic moments and the location of the n, m' and a' symmetry elements. The fractional y coordinate is given beside each atom.

3.2. Correlation with bulk magnetic measurements

Four important results therefore emerge from the refinement:

(i) the magnetic ordering arrangement below T_N: $Pnm'a(F_xC_z)$;
(ii) the magnitude of the Ho^{3+} moment at $T = 70$ mK: 5.7(2) μ_B;
(iii) the moment direction in the a–c plane: 66(1)° from [001];
(iv) the sign of the Ho^{3+} hyperfine coupling constant: positive.

Each of these can now be compared with the results of previous work.

3.2.1. The $Pnm'a'(F_xC_z)$ magnetic order is a surprising result, completely at variance with the conclusions based on previous magnetic susceptibility measurements (Bleaney *et al* 1983). Both the Curie–Weiss behaviour of the a axis susceptibility for $T > T_N$, and its rapid decrease with temperature for T just below T_N, pointed clearly to the onset of *antiferromagnetism* along the a axis. Ferromagnetism along this axis should have resulted in a susceptibility independent of temperature for $T < T_N$ so long as domain walls were free to move with the alternating magnetic field used in the susceptibility measurement (173 Hz). Lack of such freedom could have resulted in the susceptibility decrease actually observed, but such behaviour is invariably accompanied by a large loss component in the susceptibility. No such component was observed. Nevertheless, this basic disagreement points to the need for a DC susceptibility measurement below T_N. This would be expected to be temperature-independent for ferromagnetic order F_x.

3.2.2. The Ho^{3+} moment consists of a nuclear and an electronic contribution which Abragam and Bleaney define as the magnetic pseudonuclear moment and the Van Vleck electronic moment respectively.

Table 3. The structure factors contributing to the reflections measured at 70 mK.

h	k	l	$\mathcal{F}_{obs}$†	$\mathcal{F}_{cal}$‡	$\mathcal{F}_{N}$§	$\mathcal{F}_{M}$‖
1	0	0	177(2)	172	0.0000	1.7549
2	0	0	41(5)	32	0.2384	0.0418
3	0	0	167(2)	165	0.0000	1.3517
4	0	0	370(2)	343	3.5216	0.5290
5	0	0	80(1)	83	0.0000	0.6317
6	0	0	515(4)	519	6.5363	0.1213
7	0	0	70(1)	73	0.0000	0.5497
8	0	0	285(5)	282	2.3824	0.4909
9	0	0	24(3)	16	0.0000	0.1189
0	1	0	26(9)	0	0.0000	0.0000
1	1	0	186(1)	164	0.0000	1.4981
2	1	0	260(1)	232	1.1580	1.9305
3	1	0	130(1)	132	0.0000	1.0438
4	1	0	48(3)	18	0.0184	0.1364
5	1	0	117(1)	119	0.0000	0.9194
6	1	0	444(3)	415	4.3127	0.5813
7	1	0	39(1)	40	0.0000	0.3043
8	1	0	268(2)	248	2.0580	0.1596
9	1	0	46(2)	33	0.0000	0.2485
0	2	0	314(2)	346	2.3603	4.5495
1	2	0	161(2)	159	0.0000	1.3457
2	2	0	304(2)	311	3.4108	0.2166
3	2	0	155(1)	154	0.0000	1.2288
4	2	0	164(2)	172	0.3976	1.3186
5	2	0	75(4)	77	0.0000	0.5793
6	2	0	108(2)	78	0.5651	0.1684
7	2	0	66(2)	67	0.0000	0.5056
8	2	0	470(3)	484	5.2915	0.5155
9	2	0	29(3)	14	0.0000	0.1079
0	3	0	14(2)	0	0.0000	0.0000
1	3	0	153(1)	156	0.0000	1.2717
2	3	0	431(3)	468	6.2972	2.9408
3	3	0	108(3)	112	0.0000	0.8662
4	3	0	422(3)	427	4.8711	0.2425
5	3	0	100(2)	102	0.0000	0.7745
6	3	0	448(2)	437	4.5784	0.8094
7	3	0	33(3)	34	0.0000	0.2572
8	3	0	307(3)	303	2.6587	0.1684
9	3	0	31(2)	27	0.0000	0.2035
0	4	0	410(1)	454	5.2115	3.4106
1	4	0	124(1)	128	0.0000	0.9976
2	4	0	217(1)	231	1.9639	0.2100
3	4	0	121(1)	121	0.0000	0.9366
4	4	0	252(2)	231	1.1207	1.5742
5	4	0	59(4)	60	0.0000	0.4494
6	4	0	254(1)	253	2-1133	0.1980
7	4	0	53(2)	52	0.0000	0.3918
8	4	0	396(4)	413	4.1218	0.5206
0	5	0	18(8)	0	0.0000	0.0000
1	5	0	112(2)	115	0.0000	0.8807
2	5	0	270(2)	274	0.7288	2.3144
3	5	0	80(2)	81	0.0000	0.6099
4	5	0	207(1)	219	1.7835	0.2255
5	5	0	74(2)	73	0.0000	0.5540
6	5	0	406(3)	414	4.0994	0.7968

Table 3. *continued*

h	k	l	$\mathcal{F}_{obs}$†	$\mathcal{F}_{cal}$‡	$\mathcal{F}_N$§	$\mathcal{F}_M$‖
7	5	0	33(4)	24	0.0000	0.1819
8	5	0	399(4)	381	3.7018	0.1583
0	6	0	534(2)	591	8.4614	2.1931
1	6	0	83(2)	85	0.0000	0.6428
2	6	0	45(3)	42	0.2771	0.1455
3	6	0	82(1)	81	0.0000	0.6115
4	6	0	343(2)	339	2.8757	1.2341
5	6	0	41(5)	39	0.0000	0.2957
6	6	0	443(7)	476	5.1805	0.1673
7	6	0	40(4)	33	0.0000	0.2498
0	7	0	13(7)	0	0.0000	0.0000
1	7	0	78(3)	70	0.0000	0.5288
2	7	0	405(3)	401	3.7640	1.4529
3	7	0	56(4)	49	0.0000	0.3687
4	7	0	308(2)	284	2.4480	0.1547
5	7	0	44(2)	44	0.0000	0.3325
6	7	0	429(3)	423	4.2620	0.5914
0	8	0	211(3)	203	1.0836	1.2192
1	8	0	47(2)	47	0.0000	0.3574
2	8	0	379(3)	379	3.6514	0.0832
3	8	0	53(2)	45	0.0000	0.3388
4	8	0	133(2)	143	0.8090	0.7511
5	8	0	25(3)	21	0.0000	0.1588
0	9	0	17(1)	0	0.0000	0.0000
1	9	0	31(1)	35	0.0000	0.2672
2	9	0	432(3)	420	4.1837	0.7476
3	9	0	29(3)	24	0.0000	0.1827
4	9	0	342(4)	313	2.8258	0.0832
0	10	0	573(11)	668	7.3116	0.5394
1	10	0	45(3)	21	0.0000	0.1574

† $\mathcal{F}_{obs}$: square root of the observed intensities after geometrical and multiple scattering corrections have been made (arbitrary scale).
‡ $\mathcal{F}_{cal}$: scale times $(\mathcal{F}_N^2 + \mathcal{F}_M^2)^{1/2}$.
§ $\mathcal{F}_N$: modulus of the calculated nuclear structure factor, including nuclear polarisation, in units of 10^{-12} cm.
‖ $\mathcal{F}_M$: modulus of the calculated magnetic interaction vector in the same units as $\mathcal{F}_N$.

The *magnetic pseudonuclear moment*: M_I is a consequence of the enhanced nuclear Zeeman interaction arising from the hyperfine interaction, but being essentially electronic in origin, the magnetic form factor for such scattering is electronic rather than nuclear. To estimate its magnitude we refer to Bleaney *et al* 1988 who write the Hamiltonian for Ho^{3+} in HoF_3 as follows:

$$\mathcal{H} = DS_x + 2c(g_J\mu_B S_z B_z + A_j S_z I_z) - \gamma\hbar B_z I_z$$

where the z axis is chosen here to be along the crystallographic a axis. Using this Hamiltonian within an effective electronic spin $S' = \frac{1}{2}$ and nuclear spin $I = \frac{7}{2}$, their equation (4) gives eigen-energies

$$W(m_I) = \pm[D/2 + (g_J\mu_B cB_z)^2/D + \gamma'\hbar m_I B_z + Pm_I^2]$$

in which the third term in brackets is the enhanced nuclear Zeeman interaction, with

$$\gamma'/2\pi = 2A_j g_J \mu_B c^2/hD.$$

Using the appropriate values of the parameters this gives $\gamma'/2\pi = 5.158\,\mathrm{GHz\,T^{-1}}$—574 times larger than the bare Ho^{3+} nuclear moment (4.12 nuclear magnetons, or $8.98\,\mathrm{MHz\,T^{-1}}$ (Haberstroh *et al* 1972)). At temperatures below T_N, the pseudo-nuclear moment M_I due to this enhancement will therefore be $(4.12 \times 574/1836) \times \langle P\rangle_n \mu_B = 1.29\,\langle P\rangle_n \mu_B$.

Here $\langle P\rangle_n$ is the magnitude of the nuclear polarisation at temperature $T < T_N$. This value of M_I is to some extent adjustable since the experimentally determined result for $\gamma'/2\pi$ is $6.00\,\mathrm{GHz\,T^{-1}}$ (Bleaney *et al* 1988), a 16% difference from the calculated value. A better value for the pseudonuclear moment would therefore be $1.4(1)\,\langle P\rangle_n \mu_B$. Being basically electronic in origin, its contribution to the magnetic structure factor will display the same asymmetry factor and form factor as the electronic magnetic scattering. To that extent it is indistinguishable from the latter in the data fitting procedure.

The *Van Vleck electronic magnetic moment*: M_{VV} arises from the second term in the equation for the eigen-energies $W(m_I)$ given above. The value derived from magnetic susceptibility measurements along the crystallographic *a* axis (Bleaney *et al* 1988) is: $M_{VV} = 3.7(2)\mu_B$. Since the maximum possible value of this moment is $7.46\,\mu_B$ (Bleaney *et al* 1988), this corresponds to an electronic polarisation $\langle P\rangle_e = 3.7/7.46 = 0.50(1)$ at $T = 0$.

From these two terms, the predicted maximum magnitude of the Ho^{3+} moment is therefore $3.7(2) + 1.4(1) = 5.1(3)\,\mu_B$ along [100]. For the principal moment direction at 66(1)° to [001], as given by the structure refinement, this value of moment along [100] corresponds to a value of $5.1(3)/\sin(66°) = 5.6(3)\,\mu_B$ along the principal direction. This compares very well with the value obtained from the structure refinement: $5.7(2)\,\mu_B$.

3.2.3. The direction of the Ho^{3+} moment relative to [001] in the *a–c* plane receives confirmation from two quarters:

(i) Magnetic moment measurements at 0.5 K along *a* and *c* at $B = 6$ T (Bleaney *et al*) do not display complete saturation, so the calculation is not very precise. Nevertheless $M_a = 7.4\,\mu_B$, $M_c = 3.9\,\mu_B$, which is consistent with a resultant moment at $\tan^{-1}(7.4/3.9) = 62°$ to [001]. However it should perhaps be emphasised that the result obtained from the refinement *provides direct evidence of a principal moment direction at* 66(1)° *to* [001]. The moment measurements do not by themselves represent such evidence, as it was always possible that fortuitously the *a* and *c* axes just happened to be principal axes of the moment.

(ii) Zeeman optical absorption spectroscopy of the Ho^{3+} ion in HoF_3, with constant field $B = 5$ T applied as a function of angle in the *a–c* plane has shown that there is a site inequivalence consistent with the principal axes of Ho^{3+} electronic moment inclined at $66.5 \pm 2.5°$ to [001] (to be published). Again, this is in excellent agreement with the refinement value, 66(1)°, though less precise.

3.2.4. The sign of the hyperfine coupling constant is not immediately amenable to a comparison with previous experimental data. Further experiments would be necessary to confirm this result. One difficulty is that the hyperfine level splittings are determined in zero field by the pseudoquadrupole interaction, which depends on the square of the hyperfine constant A, so that for instance an analysis of the heat capacity at T just less than T_N would not help, being dependent on A^2.

3.3. Temperature dependence of scattering intensity below T_N

Four reflections were measured at some forty different temperatures between 70 mK, the base temperature of the dilution refrigerator, and 600 mK which is well above T_N.

(100) was chosen since it was believed initially, following Bleaney *et al* (1988), that the magnetic order below T_N was antiferromagnetic with Ho^{3+} electronic moments aligned along [100]. In such a case, the (100) scattering would have been due to the pseudonuclear moment alone; that is, there would have been zero contribution from either M_I or M_{VV} on account of the asymmetry parameter $[1-(\tau_z/\tau)^2]^{1/2}$. (1 4 0) and (4 2 0) were chosen as being typical of reflections whose intensity was expected to depend on both nuclear and electronic order parameters. (4 0 0) was chosen as a temperature-independent monitor of intensity since it is allowed under P*nma*, and $\mathcal{F}_{hot}$ differed from $\mathcal{F}_{cold}$ by only 1%.

Figure 2 shows the results for the (100), (140) and (420) reflections. The intensity of the (400) reflection was constant to within 3% over the several days required to complete the experiment. In the figure, all three intensities fall to zero with increasing temperature at $T = T_N = 500(5)$ mK. This is in reasonable agreement with the value of 520(10) mK determined independently from both the discontinuity in the HoF_3 heat capacity and the peak in the *a* axis susceptibility (Bleaney *et al* 1988). For purposes of theoretical analysis we assume that $T_N = 500$ mK.

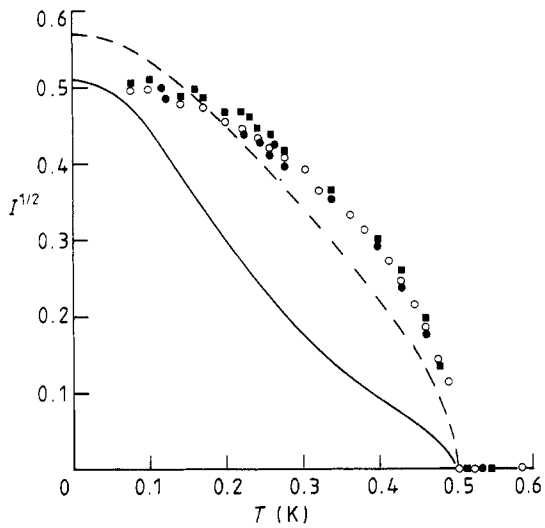

Figure 2. (Magnetic scattering intensity)$^{1/2}$ versus temperature for HoF_3; ○: data for [100], ■: [140], and ●: [420] reflections normalised to the value 0.51 at $T = 0$ K (see text). ---: $\langle P\rangle_e$, molecular field theory prediction, which tends to 0.57 at $T = 0$ K. ——: $\langle P\rangle_n$, normalised to 0.51 at $T = 0$ K (see text).

For a molecular field analysis of these data we use the formalism and notation of previous workers (Hammann and Manneville 1973). They have successfully treated similar effects in the singlet ground state systems of holmium and terbium gallium garnet ($Ho_3Ga_5O_{12}$ and $Tb_3Ga_5O_{12}$). Their Hamiltonian including the effects of the crystal field, magnetic field along [100] and magnetic hyperfine interaction is

$$\mathcal{H} = \mathcal{H}_e - g_J\mu_B J_z B_z + a_J J_z I_z$$

operating on the ground and first excited singlet states $|p, m_I\rangle$ and $|q, m_I\rangle$, with m_I the multiplicity due to the nuclear spin *I*.

Their expressions for the temperature dependence of the electronic and nuclear polarisations are

$$\langle P\rangle_e = f(B, T) = \sum_{m_I} z_0^{m_I} \sinh(\Delta'_{m_I}/T) \Big/ \sum_{m_I} \cosh(\Delta'_{m_I}/T)$$

$$\langle P\rangle_n = I_z/I = \sum_{m_I} m_I \sinh(\Delta'_{m_I}/T)/I \sum_{m_I} \cosh(\Delta'_{m_I}/T).$$

Exchange and/or dipolar interaction between electronic Ho^{3+} moments is treated in the molecular field approximation:

$$B_z^{\text{eff}} = \beta m$$

which in the above notation they write as

$$h_{\text{eff}} = xz$$

with $x = (2|w|^2/k\Delta)\beta$.

The significance of the parameter x is that it provides a criterion for deciding whether or not the nuclear-plus-electronic system will order magnetically through electronic interaction alone ($x > 1$), or whether hyperfine interaction is essential ($x < 1$).

In the notation of Bleaney *et al* (1988) the equivalent statement is that $f/\chi_{\text{true}} > 1$, where f is the molecular field correction factor defined as:

$$1/\chi_{\text{true}} = 1/\chi_{\text{meas}} + f$$

and χ_{true} and χ_{meas} are the true (i.e. calculated, interaction-free) and measured magnetic susceptibilities, respectively.

Table 4 gives the value of the various parameters defined above, both for HoF_3 (Bleaney *et al* 1988) and for $Tb_3Ga_5O_{12}$ and $Ho_3Ga_5O_{12}$ (Hammann and Manneville 1973) for comparison. It is evident that there are no adjustable parameters in any of the three systems. The HoF_3 molecular field constant β is certainly not due to dipolar interaction alone and may therefore appear to be adjustable by the addition of exchange interaction. However the calculated value of T_N can be fitted to the experimental value only by correct choice of this constant. It turns out that the calculated value is an extremely sensitive function of the parameter x—as was found by Hammann and Man-

Table 4. Values of the parameters.

	TbGaG	HoGaG	HoF_3
Δ (K)	2.87	7.4	9.48
$\lvert w\rvert/\mu_B$	6.68	7.69	8.10
$\beta(T/\mu_B)$	0.04699†	0.04768†	0.0771
$x = 2\lvert w\rvert^2\beta/k\Delta$	0.981	0.512	0.905
a_J (10^{-2} K)	2.54	3.90	3.90
$\lvert\alpha\rvert = 2\lvert w\rvert a_J/g_J\mu_B k$	0.079	0.065	0.049
T_N^{dip} (K)	0.345	0.103	—
T_N^{exp} (K)	0.25	0.19	0.515

† These are calculated from dipolar interaction. For HoF_3 the dipolar result for F_xC_z and $|w|$ as above is 0.1353 T.

neville (1973) for TbGaG and HoGaG. Therefore once the value of T_N is made to fit the experiment there are no further adjustable constants.

The calculation of the temperature dependence of both $\langle P\rangle_n$ and $\langle P\rangle_e$ is straightforward. The best-fit value of the constant $x = 0.905$ produces $T_N = 500$ mK; this value of x in turn corresponds to a molecular field constant $\beta = 0.0771$ T μ_B^{-1}.

Figure 2 shows the calculated $\langle P\rangle_n$ and $\langle P\rangle_e$ superimposed on the experimental data for the (100), (140) and (420) reflections. Here $\langle P\rangle_e$ is calculated to be 0.57 at $T = 0$, which is in reasonable agreement with the experimental result to which the three sets of data are normalised: 0.51. $\langle P\rangle_n$ is normalised to 0.51 for purposes of comparison; its temperature dependence is clearly very different from all the data sets, as expected. The temperature dependence of $\langle P\rangle_e$ can be seen to be rather different from the data, and from the corresponding temperature dependence of $\langle P\rangle_n$ it is clear that the inclusion of the appropriate degree of $\langle P\rangle_n$ dependence for each of the three reflections would not improve the fit. It must therefore be concluded that for HoF_3, molecular field theory does not provide a very satisfactory description of the temperature dependence of the order parameter $\langle P\rangle_e$ below T_N. To what extent the same is true for TbGaG and HoGaG is not known, as the previous work (Hammann and Manneville 1973) concentrated on a fit to heat capacity data only.

There are two respects in which HoF_3 differs from the other two materials TbGaG and HoGaG. First, T_N is twice as large as the larger of the two. This implies much larger inter-ionic interaction. Table 4 shows that dipolar interaction actually overestimates T_N for TbGaG, whereas for HoF_3 the dipolar interaction accounts for only 20% of the interaction constant β, and therefore plays a much less significant role. A mean field theory is therefore inherently likely to be unsatisfactory. Second, for HoF_3 there is some doubt about the correct value of the crystal field splitting (Bleaney *et al* 1988). The whole issue of the low-lying excitations in HoF_3, where the observation of unusually intense magnon sidebands implies strong pair-like electronic interaction, warrants further detailed investigation.

4. Conclusions

The magnetic ordering arrangement in HoF_3 below T_N has been determined as C_zF_x in the notation of Koehler *et al* (1960), consistent with the magnetic space group $Pnm'a'$ and the magnetic and chemical unit cells being identical. The ferromagnetic order F_x along the a axis is in complete disagreement with the antiferromagnetic order deduced from bulk magnetic measurements, and further investigation will be necessary in order to resolve this major discrepancy.

The value of T_N is determined to only $\pm 3\%$. Heat capacity measurements are usually reliable in identifying the ordering temperature but in this instance, as for HoGaG, a discontinuity rather than a well-defined peak in the heat capacity is observed. The a axis susceptibility peak occurring at 0.50 K provides independent confirmation, but is not necessarily the precise value of T_N. In the neutron measurements reported here the thermometer is not attached directly to the sample but to the cold finger of the mixing chamber. It is therefore possible for the thermometer to register a lower temperature than that of the sample. Combining these results determines T_N to be in the range 500–530 mK.

The temperature dependence of the intensities of the (100), (140) and (420) reflections for $T < T_N$ is found to agree rather poorly with the prediction of the electronic

polarisation $\langle P \rangle_e$ based on molecular field theory. This points to the need for further detailed study of the low-lying excitations that have been observed spectroscopically in HoF_3. Further work is in progress, specifically to determine the exact energies and origin of these additional excitations.

We are aware of only one other magnetic structure determination in the series of isomorphous rare earth trifluorides, namely that of TbF_3. This material orders below 3.95(5) K, and magnetisation measurements by Holmes and Guggenheim (1971) show that there is a strong ferromagnetic moment of 8 μ_B parallel to the *a* axis. These authors deduced that the structure was likely to contain Tb moments of 9 μ_B canted at an angle of 63(2) degrees to [001] in the *a–c* plane according to a C_zF_x arrangement; essentially the structure we find in HoF_3. Their suggestion was partially confirmed by powder neutron diffraction which placed the moments at 65 degrees to [001] (Piotrowski 1982). However, this refinement also included a small component of moment parallel to [010] which is forbidden in P*n*m′*a*′. Although the low symmetry of the rare earth ion site, with its nine-fold coordination by fluorine presents no obvious choice of quantum axes, it may be significant that the moment orientation is similar in both TbF_3 and HoF_3, and that, in the latter case, it is perpendicular to the shortest Ho–F bond (Ho–F2, 2.292 Å).

The form of the nuclear-plus-electronic order parameter could also be obtained independently by monitoring the resonant frequency of the ^{19}F ($I = \frac{1}{2}$) nuclei using standard NMR techniques. Likewise there is interest in a measurement of the heat capacity in the temperature range below 0.4 K, and specifically around 250 mK where a hyperfine Schottky anomaly is to be expected.

Acknowledgments

The authors would like to acknowledge the support of SERC and the hospitality of the Institute Laue Langevin, Grenoble. In particular the services of M Jean-Louis Raggazoni (ILL Cryogenics) and Mr G Read (Clarendon Sample Preparation) are applauded.

References

Becker P and Coppens P 1974 *Acta Crystallogr.* A **30** 129
Bleaney B, Gregg J F, Hill R W, Lazzouni M, Leask M J M and Wells M R 1988 *J. Phys. C: Solid State Phys.* **21** 2721
Bradley C J and Cracknell A P 1972 *The Mathematical Theory of Symmetry in Solids* (Oxford: Oxford University Press)
Brown P J and Matthewman J C 1987 *Rutherford Appleton Laboratory Report* RAL-87-010
Bukvetskii B V and Garashina L S 1977 *Koordin. Khimiya* **3** 791, 1024
Freeman A J and Desclaux 1979 *J. Magn. Magn. Mater.* **12** 11
Glattli H and Goldman M 1987 *Methods Exp. Phys.* **23** 241
Haberstroh R A, Moran T I and Penselin S 1972 *Z. Phys.* **252** 421
Hammann J and Manneville P 1973 *J. Physique* **34** 615
Holmes L and Guggenheim H J 1971 *J. Physique Coll.* **32** C1 501
Johnston D F 1966 *Proc. Phys. Soc.* **88** 37
Koehler W C, Wollan E O and Wilkinson M K 1960 *Phys. Rev.* **118** 58
Piotrowski M 1982 *Crystalline Electric Field Effects in f-electron Magnetism* ed R P Guertin *et al* (New York: Plenum) p 177
Zalkin A and Templeton D H 1953 *J. Am. Chem. Soc.* **75** 2453